**Supporting Information**

# *Helicobacter pylori* strains vary cell shape and flagellum number to maintain robust motility in viscous environments

**Laura E. Martinez[1,2**], Joseph M. Hardcastle[3**], Jeffrey Wang[2], Zachary Pincus[4], Jennifer Tsang[5], Timothy R. Hoover[5], Rama Bansil[3*], and Nina R. Salama[1,2 *]**

[1]Graduate Program in Pathobiology, Department of Global Health, University of Washington, Seattle, WA 98195 USA; [2]Division of Human Biology, Fred Hutchinson Cancer Research Center, Seattle, WA 98109 USA; [3]Department of Physics, Boston University, Boston, MA 02215 USA; [4]Department of Developmental Biology and Department of Genetics, Washington University School of Medicine, St. Louis, MO 63110, USA; [5]Department of Microbiology, University of Georgia, Athens, GA 30602, USA. **L.E.M. and J.M.H. contributed equally to the research as first co-authors.

**Corresponding Authors:** *Nina R. Salama**,** Fred Hutchinson Cancer Research Center, 1100 Fairview Ave. N, Mailstop C3-168, Seattle, WA 98109-1024, USA. Phone: 206-667-1540. Fax: 206-667-6524. Email: nsalama@fhcrc.org

*Rama Bansil, Department of Physics, Boston University, 590 Commonwealth Avenue, Boston, MA 02215, USA. Phone: 617-353-2969. Fax 617-353-9393. Email: rb@bu.edu

**Supporting information inventory:**

**Table S2.** Primers used in this study.

**Table S3.** Percent track linearity for wild-type and straight rod mutants swimming in broth and viscous media.

**Table S4.** Average cell body and helical parameters of flagellar mutants.

**Supplemental figures:**

**Figure S1.** Individual cell trajectories of tracked bacteria show diverse swimming patterns.

**Figure S2.** Wild-type *H. pylori* speed distributions reflect temporal variation of individual bacteria in broth and a gel-like PGM solution.

**Figure S3.** Straight rod mutants show similar flagella parameters to wild-type *H. pylori*.

**Figure S4.** Deletion of *csd6* results in straight rod morphology in the PMSS1 strain background.

**Figure S5.** Straight rods show increased fractions of immobilized bacteria in viscous PGM media.

**Figure S6.** Straight rods show similar temporal variation in swimming speed to wild-type in broth and a gel-like PGM solution.

**Figure S7.** Flagellar mutants display increased cell length and helical parameters relative to wild-type B128.

**Videos 1 – 4. Related to Figs 4 and 5.**

Video 1. The motility of wild-type LSH100 suspended in a viscous solution of PGM at 15 mg $mL^{-1}$.

Video 2. The motility of LSH100 Δ*csd6* straight rods suspended in a viscous solution of PGM at 15 mg $mL^{-1}$.

Video 3. The motility of wild-type PMSS1 suspended in a viscous solution of MC at 10 mg $mL^{-1}$.

Video 4. The motility of PMSS1 Δ*csd6* straight rods suspended in a viscous solution of MC at 10 mg $mL^{-1}$.

**Videos 5 - 6. Related to Figs 8 and 9.**

Video 5. The motility of wild-type B128 suspended in a viscous solution of PGM at 15 mg $mL^{-1}$.

Video 6. The motility of B128 sRNA_T flagellar mutant suspended in a viscous solution of PGM at 15 mg $mL^{-1}$.

**Table S1. Bacterial strains used in this study**

| Strain Name | Genotype or Description | Shape phenotype | Reference or Source |
|---|---|---|---|
| LSH100 | Wild-type *H. pylori*, NSH57 *fliM* mutation repaired | helical | Lowenthal *et al*., 2009 |
| B128 | Wild-type *H. pylori* | helical | Mc Clain *et al*., 2009 |
| PMSS1 | Wild-type *H. pylori* | helical | Lee *et al*., 1997; Arnold *et al*., 2011 |
| TSH17 | Δ*csd6::cat* in LSH100 | straight | Sycuro *et al*., 2013 |
| LMH6 | Δ*csd6::cat* in PMSS1 | straight | This study |
| LMH9 | Δ*motB::tn* in LSH100 | helical | Salama *et al*., 2004; This study |
| $fliO_{\Delta C}$ | $fliO_{\Delta C}$ in B128 C-terminal deletion: amino acids 217 to 283 were replaced with a FLAG tag | helical | Tsang and Hoover, 2014 |
| sRNA_T | sRNA_T::aphA-3 in B128 | helical | This study |

**Table S2.** Primers used in this study

| ***Targeted disruption primers*** | | | |
|---|---|---|---|
| **Gene name** | ***H. pylori* gene annotation** | **Primer** | **Sequence** |
| *csd6* | HPG27_477[a] (HP0518)[b] | 476F | gcgcgctctagAAGGAAGAAAAGAGCTTGC[c] |
| | | 478R | GCTGGTAGGCTTTGTAATC |
| *motB* | HPG27_772[a] (HP0816)[b] | 771F | TCATTATCATCGTGCCTA |
| | | 773R | AAATTGGTGCTCACTTCT |
| **Name** | **HPnc Number/ Alternative ID** | | **Sequence** |
| sRNA_T | HPnc7700; Adjacent gene HP1439[b]/HPr07 (16S rRNA)) | sRNA_T up F | AGT TTC ACA GCG CAT TAT AAG |
| | | sRNA_T up R | GTA TAA CAT AGT ATC GAC TGA CAA GTT TGA TGA GCA GGA |
| | | sRNA_T down F | GAA TTG TTT TAG TAC CTA GGC GAA TGT TAA AAG CTT TTC TC |
| | | sRNA_T down R | ATA CAC GAA GAA CCT TAC CTA |
| | | kan F | GTC GAT ACT ATG TTA TAC |
| | | kan R | CTA GGT ACT AAA ACA ATT C |

[a]Gene annotation in the human clinical isolate G27 (Baltrus *et al*., 2009).
[b]Gene annotation in the human clinical isolate 26695 (Tomb *et al*., 1997).
[c]Gene specific sequences are in uppercase and sequences added for cloning are in lower case.

**Table S3.** Percent track linearity for wild-type and straight rod mutants swimming in broth and viscous media.

| Solution | Strain | | n | Average %TL | K-S p-value[c] for %TL |
|---|---|---|---|---|---|
| **BB10** | | **B128** | 99 | 59% | |
| | **LSH100** | **WT** | 100 | 54% | 0.468 |
| | | **Δ*csd6*** | 100 | 57% | |
| | **PMSS1** | **WT** | 100 | 67% | 0.024 |
| | | **Δ*csd6*** | 100 | 60% | |
| **PGM[a] 15 mg mL$^{-1}$** | | **B128** | 100 | 77% | |
| | **LSH100** | **WT** | 100 | 81% | 0.281 |
| | | **Δ*csd6*** | 100 | 78% | |
| | **PMSS1** | **WT** | 100 | 89% | 0.367 |
| | | **Δ*csd6*** | 100 | 87% | |
| **PGM 30 mg mL$^{-1}$** | | **B128** | 100 | 74% | |
| | **LSH100** | **WT** | 100 | 82% | 0.581 |
| | | **Δ*csd6*** | 100 | 78% | |
| | **PMSS1** | **WT** | 100 | 83% | 0.367 |
| | | **Δ*csd6*** | 100 | 81% | |
| **MC[b] 10 mg mL$^{-1}$** | **LSH100** | **WT** | 100 | 68% | 0.581 |
| | | **Δ*csd6*** | 100 | 66% | |
| | **PMSS1** | **WT** | 100 | 81% | 0.699 |
| | | **Δ*csd6*** | 100 | 77% | |
| **MC 15 mg mL$^{-1}$** | **LSH100** | **WT** | 100 | 56% | 0.010 |
| | | **Δ*csd6*** | 100 | 69% | |
| | **PMSS1** | **WT** | 48 | 81% | 0.687 |
| | | **Δ*csd6*** | 48 | 76% | |

[a]PGM: Purified gastric mucin at pH 6.0.
[b]MC: Methylcellulose.
[c]K-S test used to compare WT to mutant percent track linearity (%TL); p-values < 0.05 are considered significant.

**Table S4.** Average cell body and helical parameters of flagellar mutants.

| Strain | Average cell body parameters from Cell Tool[a] | | | | Average helical parameters[b] | | |
|---|---|---|---|---|---|---|---|
| | n | Cell length (μm) | Side Curvature | Cell diameter (μm) | n | Helical radius (μm) | Helical pitch (μm) |
| **Wild-type B128** | 274 | 2.82 | 3.08 | 0.58 | 272 | 0.10 | 2.4 |
| **B128 *fliO*$_{\Delta C}$** | 307 | 3.25 | 3.98 | 0.66 | 296 | 0.17 | 2.6 |
| **B128 sRNA_T** | 326 | 3.41 | 3.94 | 0.60 | 305 | 0.14 | 2.5 |

[a]Cell body measurements acquired from CellTool.
[b]Helical parameter measurements acquired from fitting centerlines to a sinusoid.

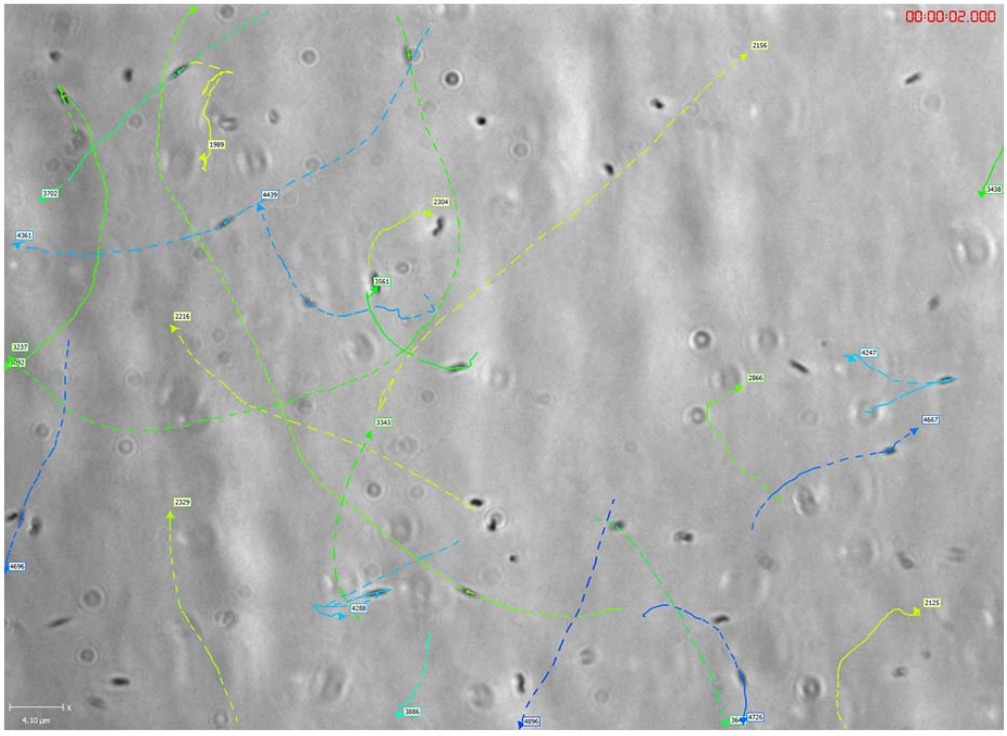


**Figure S1. Individual cell trajectories of tracked bacteria show diverse swimming patterns**. Snapshot images were superimposed with the tracks (including track identification numbers) acquired from the entire video for individual wild-type bacteria (LSH100) tracked by live-cell video microscopy, swimming in a viscous solution of PGM (15 mg $mL^{-1}$). Videos were obtained at 60X and recorded at 100 ms intervals over a 10 s period (10 fps). Videos were then uploaded to Volocity (v6.1) to track individual bacterial cells according to size (area ($\mu m^2$)) and pixel intensity (see Experimental Procedures). Each single cell tracked was visually inspected to exclude bacteria that displayed less than 1.5 μm in displacement, and overlapping tracks for the same bacterial cell or joined tracks between bacteria were discarded. As shown, some bacteria swim in relatively straight lines, others in loose or tight curves, and some reverse direction.

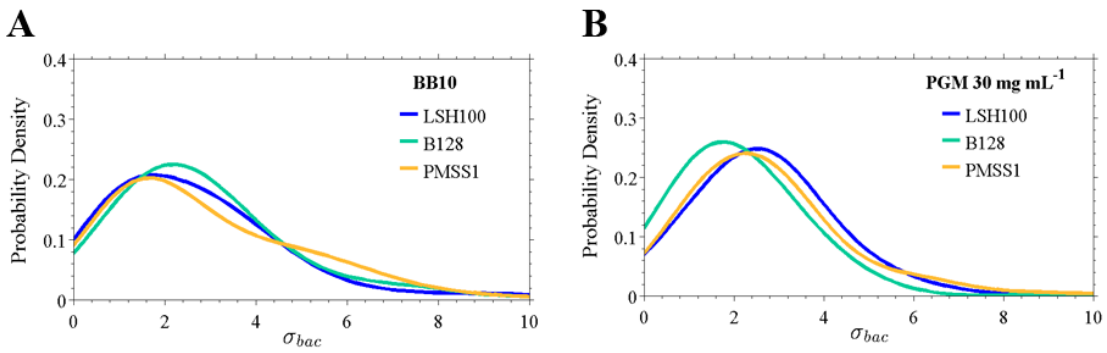


**Figure S2. Wild-type *H. pylori* speed distributions reflect temporal variation of individual bacteria in broth and a gel-like PGM solution.** (A) Smooth histograms summarizing the standard deviation distributions acquired for each individual bacterium's speed trajectory, $\sigma_{bac}$, of LSH100, B128, and PMSS1 in broth (BB10) (A) and in PGM solutions at 30 mg $mL^{-1}$ (B). In BB10, all strains show similar distributions: K-S p=0.46 for LSH100 vs. B128; K-S p=0.57 for LSH100 vs. PMSS1; and K-S p=0.28 for B128 vs. PMSS1. In PGM 30 mg $mL^{-1}$, LSH100 and PMSS1 show similar temporal speed variation distributions (K-S p=0.89), while B128 shows a significantly different temporal speed variation distribution from both strains ($p<0.05$).

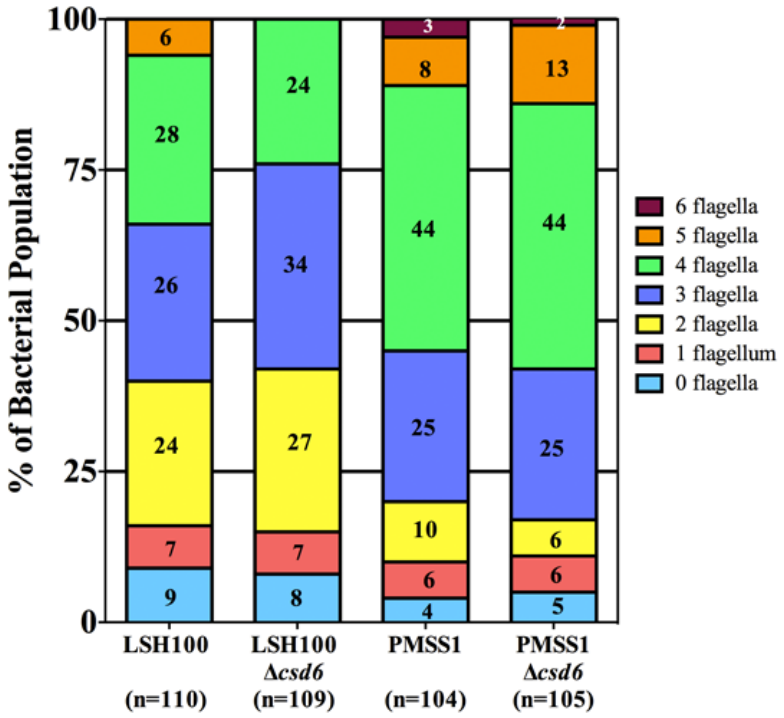


**Figure S3. Straight rod mutants show similar flagellum parameters to wild-type *H. pylori*.** Individual bacteria for wild-type LSH100 and PMSS1 and their respective isogenic straight rods mutants were analyzed for the number of flagella from TEM images and are reported as percent of the total bacterial population examined (n=104-110).

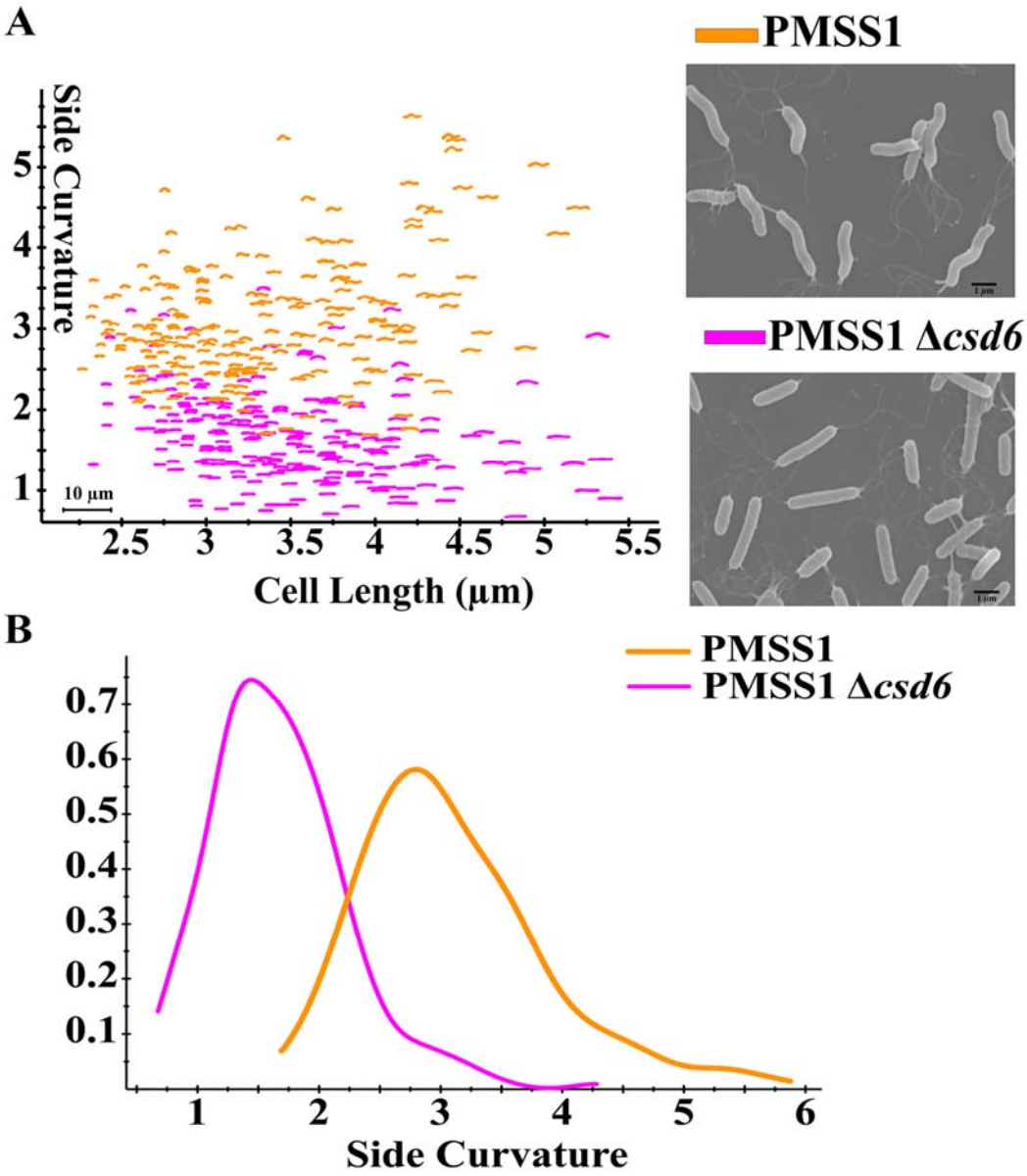


**Figure S4. Deletion of *csd6* results in straight rod morphology in the PMSS1 strain background.** (A) Scatter plot of side curvature vs. cell length (µm) for wild-type PMSS1 (n=222) and the *csd6* targeted deletion mutant generated in the PMSS1 strain background (n=228). Each point represents the outline of individual bacteria captured by phase contrast microscopy (100X). Inset panel: SEM images of PMSS1 (top) and PMSS1 Δ*csd6* (bottom). Scale bar = 1 µm. (B) Smooth histogram of side curvature frequency distribution of the same populations shown in A. Statistical test of the Kolmogorov-Smirnov (K-S) distance shows p <0.00001 for side curvature distributions.

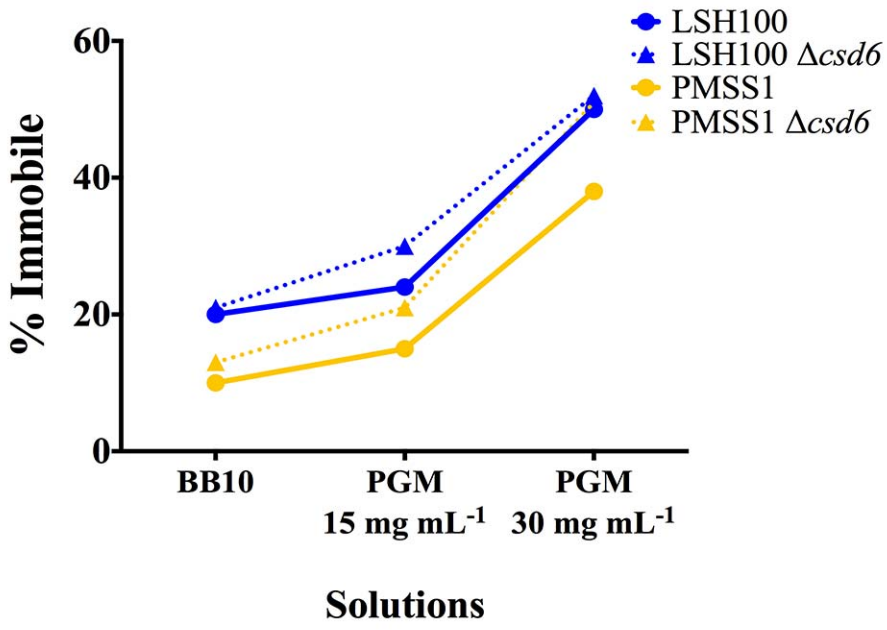


**Figure S5. Straight rods show increased fractions of immobilized bacteria in viscous PGM media.** The percentage of immobilized bacteria was calculated by dividing the total number of nonmotile cells (bacteria that exhibit displacements < 0.3 μm) by the total bacterial population examined, as described in the Experimental Procedures. Data shown are from the same experiments in Figures 5-7 and Table 3.

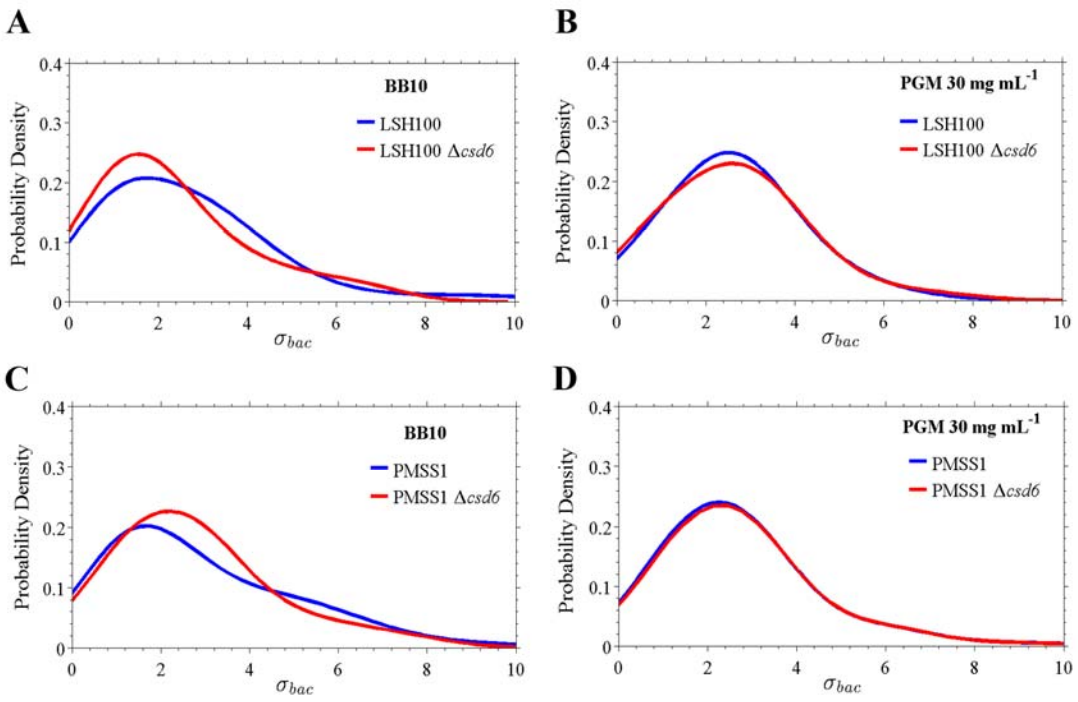


**Figure S6. Straight rods show similar temporal variation in swimming speed to wild-type in broth and a gel-like PGM solution.** Smooth histograms summarizing the standard deviation distributions acquired for each individual bacterium's speed trajectory, $\sigma_{bac}$, of wild-type *H. pylori* strains and isogenic Δ*csd6* straight rod mutants in LSH100 (A,B) and PMSS1 (C,D) strains in broth (BB10) and in gel-like PGM solutions at 30 mg $mL^{-1}$. The distributions show similar temporal speed variation profiles between wild-type and straight rod mutants, where K-S p = 0.14 (broth) and p = 0.79 (PGM at 30 mg $mL^{-1}$) for LSH100 vs. LSH100 Δ*csd6*, and p = 0.34 (broth) and p = 0.19 (PGM at 30 mg $mL^{-1}$) for PMSS1 vs. PMSS1 Δ*csd6.*

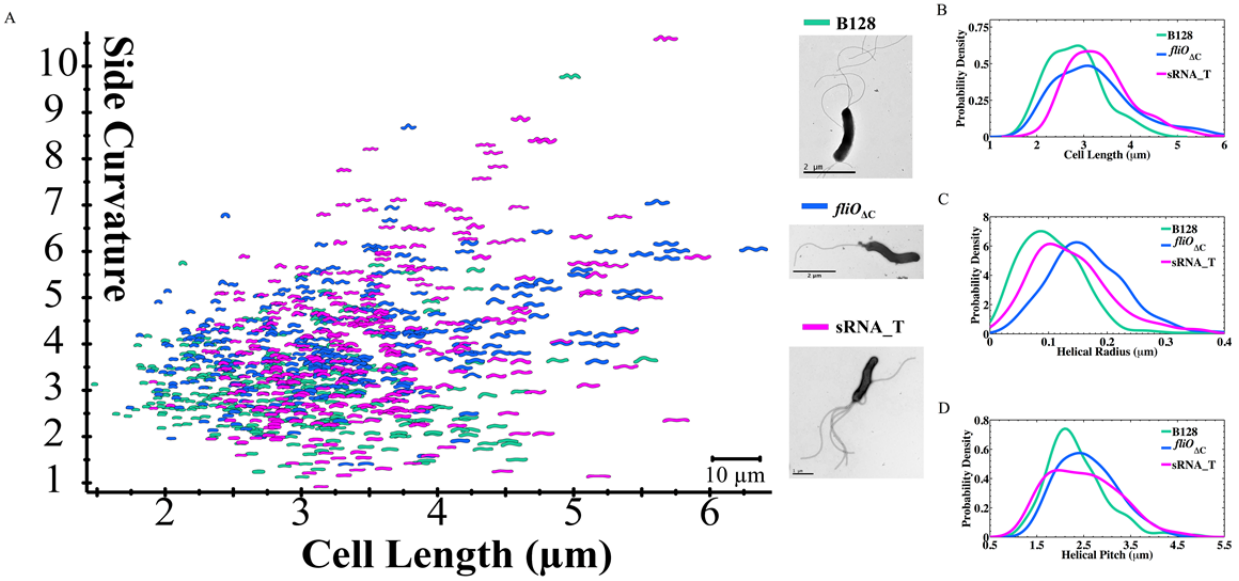


**Figure S7. Flagella mutants display increased cell length and helical parameters relative to wild-type B128.** (A) Side curvature vs. cell length (μm) of individual bacterial cells imaged by phase contrast microscopy for B128 (n=274), *fliO*$_{\Delta C}$ (n=307), and sRNA_T (n=326) bacteria. Inset panel: TEM images of each. Scale bar = 1 μm for sRNA_T and 2 μm for B128 and *fliO*$_{\Delta C}$. Data shown are morphology analyses from two independent cultures for each strain. (B-D) Smooth histograms summarizing probability density distributions of cell length (μm) (B), helical radius (μm) (C), and helical pitch (μm) (D) measurements acquired for wild-type B128 (n=272), *fliO*$_{\Delta C}$ (n=296), and sRNA_T (n=305).

## References


Arnold, I.C., Lee, J.Y., Amieva, M.R., Roers, A., Flavell, R.A., Sparwasser, T., and Müller, A. (2011) Tolerance rather than immunity protects from *Helicobacter pylori*-induced gastric preneoplasia. *Gastroenterology* **140(1):** 199-209.

Baltrus, D.A., Amieva, M.R., Covacci, A., Lowe, T.M., Merrell, D.S., Ottemann, K.M., *et al.* (2009) The complete genome sequence of *Helicobacter pylori* strain G27. *J. Bacteriol.* **191(1):** 447-448.

Lee, A., O'Rourke, J., De Ungria, M.C., Robertson, B., Daskalopoulos, G., and Dixon, M.F. (1997) A standardized mouse model of *Helicobacter pylori* infection: introducing the Sydney strain. *Gastroenterology* **112(4):** 1386-1397.

Lowenthal, A.C., Hill, M., Sycuro, L.K., Mehmood, K., Salama, N.R., and Ottemann, K.M. (2009) Functional analysis of the *Helicobacter pylori* flagellar switch proteins. *J. Bacteriol.* **191(23):** 7147-7156.

McClain, M.S., Shaffer, C.L., Israel, D.A., Peek, Jr., R.M., and Cover, T.L. (2009) Genome sequence analysis of *Helicobacter pylori* strains associated with gastric ulceration and gastric cancer. *BMC Genomics* **10:** 3.

Salama, N.S., Shepherd, B., and Falkow, S. (2004) Global Transposon Mutagenesis and Essential Gene Analysis of *Helicobacter pylori*. *J. Bacteriol.* **186(23):** 7926-7935.

Sycuro, L.K., Rule, C.S., Petersen, T.W., Wyckoff, T.J., Sessler, T., Nagarkar, D.B., *et al.* (2013) Flow cytometry based enrichment for cell shape mutants identifies multiple genes that influence *Helicobacter pylori* morphology. *Mol. Microbiol.* **90(4):** 869-83.

Tomb, J.F., White, O., Keriavage, A.R., Clayton, R.A., Sutton, G.G., Fleischmann, R.D., *et al.* (1997) The complete genome sequence of the gastric pathogen *Helicobacter pylori*. *Nature* **388 (6642):** 539-47.

Tsang, J. and Hoover, T.R. (2014) Requirement of the flagellar protein export apparatus component FliO for optimal expression of flagellar genes in *Helicobacter pylori. J. Bacteriol.* **196(15):** 2709-17.

Volocity: Improvisation PE. 2011. Volocity 3D Rendering and Image Analyses Program. Version 6.1.